Turbulent Spot/Separation Bubble Interactions in a Spatially Evolving Supersonic Boundary-Layer Flow

L Krishnan and N D Sandham
Aeronautics & Astronautics
School of Engineering sciences
University of Southampton, Southampton
SO17 1BJ, United Kingdom

n.sandham@soton.ac.uk

ABSTRACT

The growth and breakdown of localised disturbances into a turbulent spot in a Mach 2 boundary-layer flow have been investigated by direct numerical simulation. In particular, the interaction of a turbulent spot with a shock-induced separation bubble is studied. The primary vortex structures triggered by the injected low momentum fluid and the metamorphosis of the hairpin structures into a turbulent spot are clearly identified in the present study. The spot-separation bubble interaction is found to enhance the breakdown of the hairpin structures i.e. is capable of advancing the transition process. A substantial increase in the lateral spreading of the spot is observed due to the spot/bubble interaction. Locally averaged profiles of the flow quantities within the spot show behaviour similar to developed turbulent flows.

1 INTRODUCTION

Understanding complex flow physics like laminar-to-turbulent transition and shock/boundary-layer interactions is of great importance in the design and development of flight vehicles at hypersonic speeds, but prediction of the extremely high local variation of the fluid properties associated with the transition process remains a difficult task. The boundary layer associated with an aerodynamic configuration can be laminar and stable, laminar but unstable, intermittently turbulent, or fully turbulent. The laminar base flow can be perturbed using various forcing techniques like vibrating ribbons, acoustic forcing, localised point source disturbances (loud speakers, sparks), suction/blowing slots, roughness elements and complex wave generators. The growth of instabilities in a laminar flow triggers the transition process and intermittent turbulent regions, generally referred as turbulent spots, may occur in the flow. The growth and merging of these turbulent spots results in a fully developed turbulent flow field. Intrusion of large amplitude non-linear perturbations may skip the linear stages of transition in a process known as bypass transition. The extent of the transition length is generally shorter in a bypass transition scenario. A detailed study of the dynamics of turbulent spots can also be useful in extending our understanding of turbulence physics.

The length of the transition region mainly depends on spot characteristics such as the convective speed of the leading and trailing edges of the spot, lateral growth rate and interactions between spots. A schematic of a turbulent spot is depicted in Figure 1.a and 1.b. A side view of a spot (Figure 1.a) shows the main spot features: 1) leading edge overhang, 2) spot core or body and 3) the trailing interface. A more detailed description of a spot is given in Figure 1.b (Plan view), showing 1] spot spreading half-angle; 2] spanwise wings; 3] streaks; 4] spot core; 5] spot leading interface; 6] spot front tip; 7] oblique waves; 8] lateral breakdown

Paper presented at the RTO AVT Specialists' Meeting on "Enhancement of NATO Military Flight Vehicle Performance by Management of Interacting Boundary Layer Transition and Separation", held in Prague, Czech Republic, 4-7 October 2004, and published in RTO-MP-AVT-111.

Report Documentation Page

Form Approved
OMB No. 0704-0188

1. REPORT DATE	2. REPORT TYPE	3. DATES COVERED
01 OCT 2004	**N/A**	**-**

4. TITLE AND SUBTITLE	5a. CONTRACT NUMBER
Turbulent Spot/Separation Bubble Interactions in a Spatially Evolving Supersonic Boundary-Layer Flow	5b. GRANT NUMBER
	5c. PROGRAM ELEMENT NUMBER
6. AUTHOR(S)	5d. PROJECT NUMBER
	5e. TASK NUMBER
	5f. WORK UNIT NUMBER
7. PERFORMING ORGANIZATION NAME(S) AND ADDRESS(ES) **Aeronautics & Astronautics School of Engineering sciences University of Southampton, Southampton SO17 1BJ, United Kingdom**	8. PERFORMING ORGANIZATION REPORT NUMBER
9. SPONSORING/MONITORING AGENCY NAME(S) AND ADDRESS(ES)	10. SPONSOR/MONITOR'S ACRONYM(S)
	11. SPONSOR/MONITOR'S REPORT NUMBER(S)

12. DISTRIBUTION/AVAILABILITY STATEMENT
Approved for public release, distribution unlimited

13. SUPPLEMENTARY NOTES
See also ADM201868, RTO-MP-AVT-111 Enhancement of NATO Military Flight Vehicle Performance by Management of Interacting Boundary Layer Tranisition and Separation (L'amelioration des performances des vehicules aeriens militaires de l'OTAN par la gestion de l'interaction entre la transition et le decollement de la couche limite)., The original document contains color images.

14. ABSTRACT

15. SUBJECT TERMS

16. SECURITY CLASSIFICATION OF:			17. LIMITATION OF ABSTRACT	18. NUMBER OF PAGES	19a. NAME OF RESPONSIBLE PERSON
a. REPORT	b. ABSTRACT	c. THIS PAGE			
unclassified	**unclassified**	**unclassified**	**UU**	**16**	

Standard Form 298 (Rev. 8-98)
Prescribed by ANSI Std Z39-18

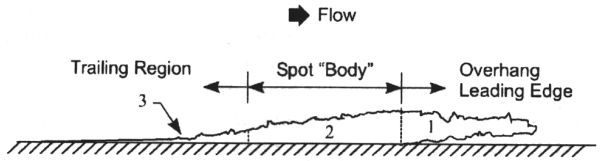

Figure 1.a: Schematic outline of a turbulent spot [Gad-El-Hak (1981)]

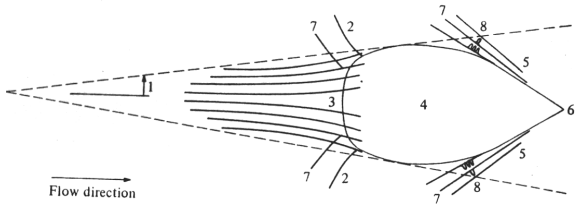

Figure 1.b: Turbulent spot nomenclature [Carlson *et al.* (1982)]

A detailed review of transition studies and turbulent spots in a variety of flows was given by Narasimha (1985). Flow visualisation experiments of Perry *et al.* (1981) suggested a turbulent spot to be an array of Λ-shaped vortices (substructures). Sankaran *et al.* (1988) studied the characteristics of substructures within a turbulent spot in a slightly heated laminar boundary layer flow. They found that the number of substructures in the spot increases with streamwise distance, resulting in the streamwise growth of the spot, and that the new substructures are formed near the trailing edge of the spot. Gad-El-Hak *et al.* (1981) investigated the transition on a flat plate. Their experiments showed that the growth rate of turbulent spots in the lateral direction by destabilisation of the surrounding laminar boundary layer is an order of magnitude greater than the growth rate normal to the wall. Sabatino *et al.* (2002) experimentally investigated the properties of artificially triggered turbulent spots in a heated laminar boundary layer in a water channel facility. They found that the highest surface heat transfer occurred in the trailing region of the spot, whereas entrainment and recirculation of warm surface fluid within the spot body resulted in reduced effective heat transfer.

Narasimha (1985) reported the influence of pressure gradients on the geometry of a spot, its propagation characteristics and spreading. His results showed that an adverse pressure gradient has a destabilising effect, while a favourable pressure gradient delays the transition process. His intermittency distributions also revealed sub-transitions within the transition zone. The visualisation experiments of Zhong *et al.* (2000) in an incompressible flow also confirmed the increase in the spot lateral spreading with increasing adverse pressure gradients.

Variation of the wall and lateral spreading angles of the disturbance region with local Mach number was reported by Fischer (1972). He summarized the results of earlier investigations on disturbance growth. The spreading angle relative to the wall remained invariant with Mach number while the lateral spreading angle decreased sharply from 11 degrees to 3 degrees with increasing Mach number up to about Mach 6.0. The recent boundary layer transition measurements by Mee (2002) in hypervelocity flows (Mach 6) also showed that turbulent spots grow at a much lower lateral spreading angle than at low Mach numbers.

Kleiser and Zang (1991) reviewed the previous numerical studies on transition to turbulence, which are mainly confined to incompressible flow. Data for compressible spots in the literature is very limited. Krishnan and Sandham (2004) studied the growth of turbulent spots in a compressible channel flow using

a mixed-time-scale large-eddy simulation model. They found that increase in the Mach number has a stabilizing effect on the growth of the disturbances while an increase in the Reynolds number enhanced the spot growth. Dolling (2001) in his review on shock-wave/boundary layer interactions clearly discussed the progress made in the past and potential areas to explore in the future. He suggested that a careful study of the influence of transitional boundary layers on shock wave/boundary-layer interactions may shed light on the peak heating rates, global flowfield unsteadiness and the underlying complex turbulence physics.

Most of the research to date has been performed to study either the transition process or shock/turbulence interactions separately. Less work has been done to study the dynamics of a turbulent spot interacting with a separation bubble in the compressible flow regime. The primary interest of the present contribution is to simulate a practically relevant complex flow condition in which a turbulent spot in a boundary layer near transition is simultaneously undergoing interaction with a separation bubble induced by an impinging oblique shock.

2 SPOT SIMUATIONS

2.1 Numerical Approach

The governing equations are solved using a stable high-order scheme that is free from upwinding and any other explicit artificial dissipation terms. An entropy splitting approach is used to split the Euler terms. All the spatial discretizations are carried out using a fourth-order central-difference scheme while the time integration uses a third-order Runge-Kutta method. A stable boundary scheme of Carpenter (1999), along with a Laplacian formulation of the viscous and heat conduction terms, are used to prevent any odd-even decoupling associated with central schemes. An artificial compression method (ACM) variant of a standard total variation diminishing (TVD) family is used to capture flow discontinuities. More details regarding the entropy-splitting and other numerical issues used in the present scheme can be found in Sandham *et al.* (2002).

2.2 Flow Details

The flow domain is a box of dimensions 600 x 30 x 60 in the streamwise *(x),* wall normal *(y)* and spanwise *(z)* directions respectively. All the lengths are normalised with the displacement thickness (δ^*_{in}) of the laminar inflow profile. The laminar base flow is obtained by a separate self-similar compressible boundary layer solution. Details of the various test cases considered are given in Table 1. For the present flow conditions an unperturbed laminar base flow remained laminar. The flow domain is discretized using an equally spaced grid along the streamwise and spanwise directions and a stretched grid in the wall normal direction. In the supersonic part of the inflow boundary all the properties are fixed, while in the subsonic region the pressure is extrapolated from the interior. Characteristic non-reflective conditions at the outlet, integrated characteristic boundary condition at the top surface and a no-slip, isothermal condition at the flat plate surface are imposed as boundary conditions. Periodic boundary conditions are applied in the spanwise direction. The variation of the dynamic viscosity with temperature is included by using a power law with an exponent of 2/3. For the spot/separation bubble interaction case an oblique shock was introduced on the upper boundary with an incident shock angle of 32.58 degrees such that it impinges approximately at x =137 at the lower boundary. The static pressure ratio, i.e. ratio of pressure after the shock reflection to pressure before the shock impingement is taken as 1.4. First the laminar base flow is allowed to develop along the plate until steady-state conditions are reached. Then the shock conditions are imposed at the upper boundary. The solution is advanced until the change in the dimensions of the separation bubble with time is negligible.

Case	Mach No.	$Re_{\delta^*_{in}}$	T_w / T_∞	L_x / δ^*_{in}	L_y / δ^*_{in}	L_z / δ^*_{in}	N_x	N_y	N_z
M2S/M2SSI	2	950	1.672	600	30	60	601	101	121

Table 1: Details of the spot cases

2.2 Spot Initialization

The spatially developed laminar base flow is perturbed by a localised injection of low momentum fluid through the flat plate surface. A spanwise symmetric rectangular slot of dimensions 4 x 4 (x, z) is used. The low momentum fluid is injected for a short duration of 8 non-dimensional time units (δ^*_{in} / u_∞) by specifying vertical velocity at the plate surface as

$$v_{inj} = 0.2\, u_\infty \quad \text{for} \quad 20 \le x \le 24 ; 28 \le z \le 32 ; \text{and } t < 8$$

$$= 0 \qquad \text{otherwise,}$$

where u_∞ is the free stream velocity and v_{inj} is the velocity of the injected fluid. The amplitude of the disturbance is chosen such that a spot can be triggered and tracked within the present domain size.

3 MACH 2 SPOT RESULTS (M2S)

3.1 Evolution of Spot Structures

Coherent structures in the flow are identified by calculating the second invariant $(\Pi = (\partial u_i / \partial x_j) * (\partial u_j / \partial x_i))$ of the velocity gradient tensor. Negative values of Π correspond to regions in the flow where the vorticity dominates over strain. The injected low momentum fluid acts as a blockage to the flow and induces a hairpin vortex downstream of the injection slot. This primary hairpin structure is stretched by the mean flow shearing action and is convected downstream. If the strength of this primary structure is high it triggers second-generation hairpin structures and quasi-streamwise vortices and other auxiliary structures in the flow. With further growth and interaction these complex flow structures finally evolve into the localised turbulent patch shown in Figure 2, i.e. a turbulent spot. The evolved spot at time t = 228 is found to have an arrowhead shape with a leading edge overhang and looks similar to spots in incompressible flows. Plan and side views of the integrated three dimensional surface contours of the wall normal vorticity are shown in Figure 3, clearly illustrating the turbulent core region, arrowhead shaped front and the overhang region of the spot. It is interesting to note that the spanwise symmetries have not yet broken down even though complex flow structures are present inside the spot.

Perry *et al.* (1981) in their visual study of turbulent spots in incompressible flows showed that a turbulent spot is an array of Λ-shaped vortices (Figure 4). The organisation of spot structures during the early stages of transition (t = 228) shows a good agreement with their conceptual model. Further (broadly self-similar) growth of the spot as it is convected downstream results in the breakdown of spanwise symmetries in the rear part of the spot due to chaotic (non-linear) interactions of the spot substructures. Figure 5 shows the top and side views of a well developed turbulent spot at t = 468.

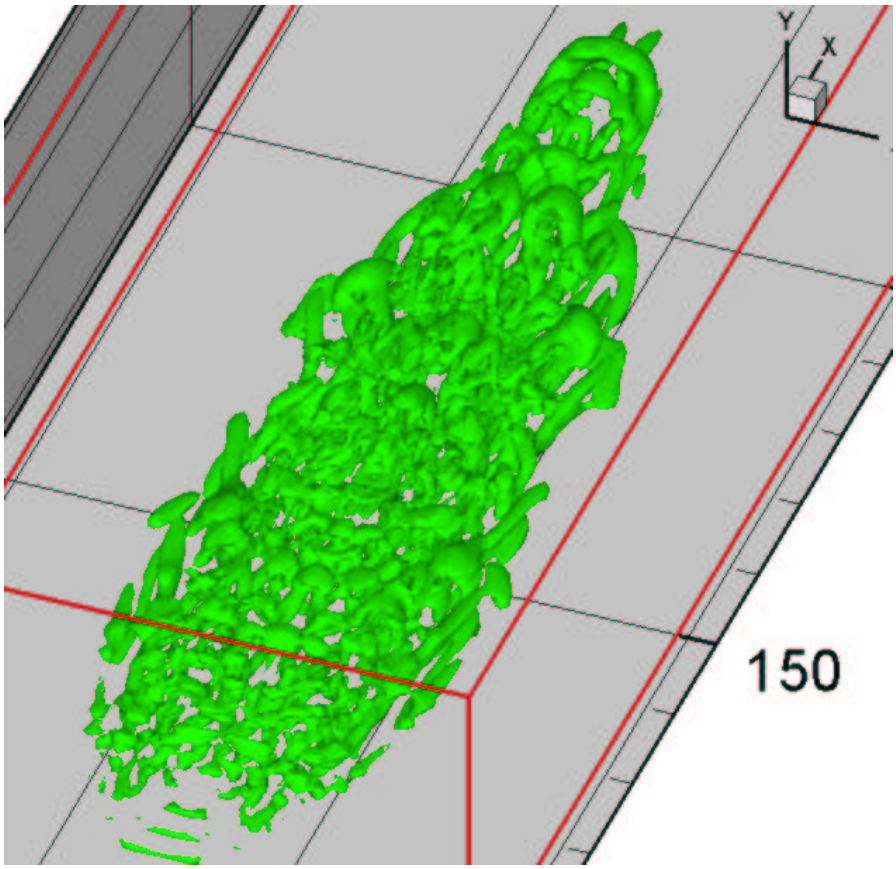

Figure 2: Iso surface of the second invariant ($\prod = -0.003$) at t = 228

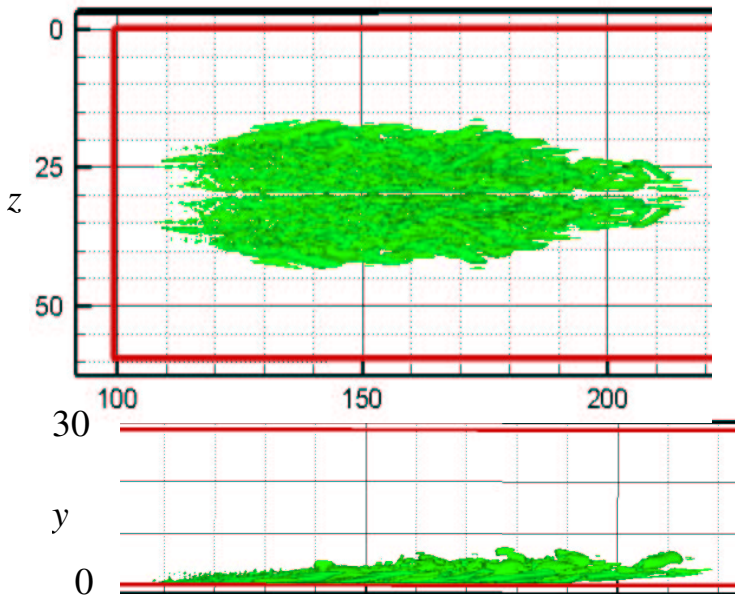

Figure 3: Iso surface of wall-normal vorticity (+0.06, - 0.06)

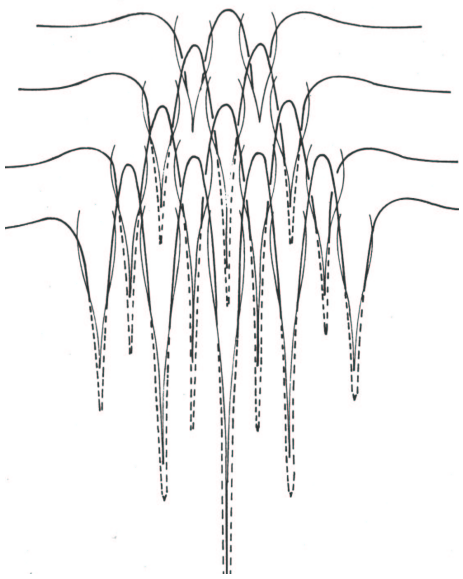

Figure 4: Conceptual model of hairpin structures evolving into a spot (Perry *et al.*)

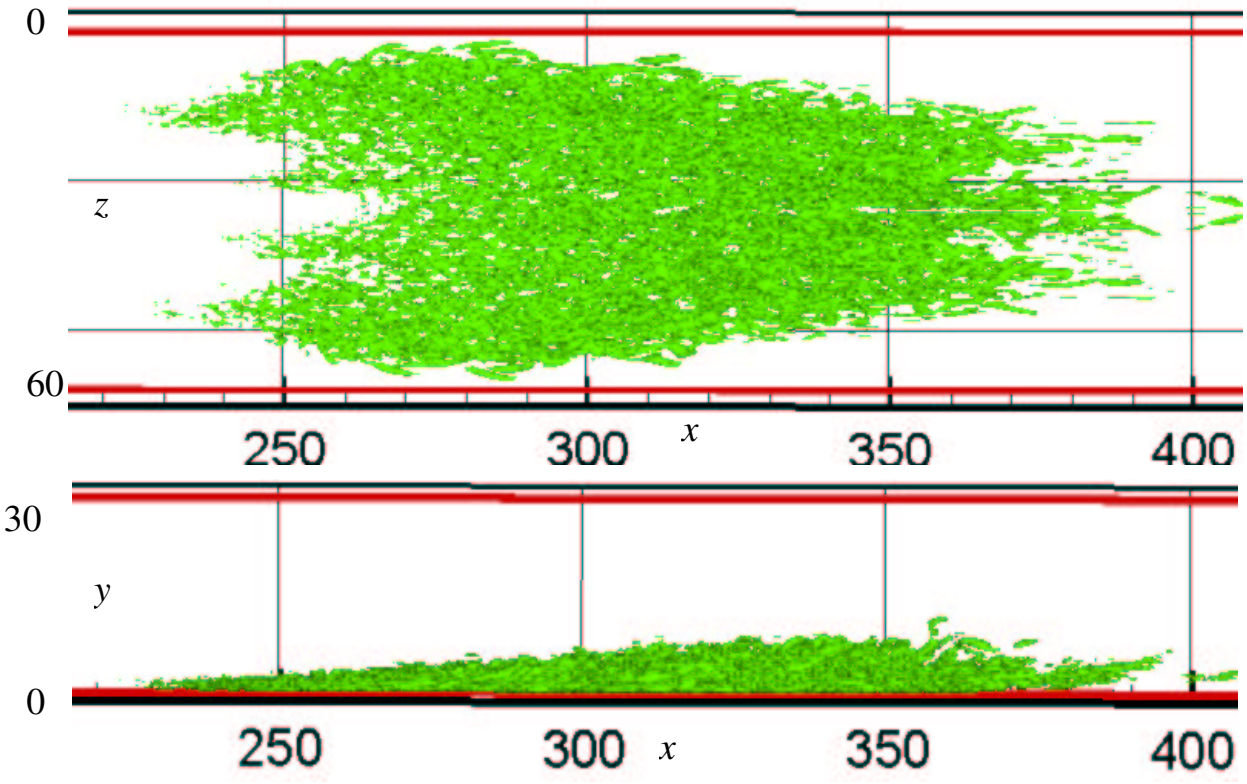

Figure 5: Top and side view of a developed turbulent spot at t = 468

Another striking feature that can be observed from all the plots is the region behind the spot, showing no signs of turbulent flow. This region is generally termed as "calmed region". The reason for this suppression of the perturbations in the wake of a spot is not fully explained. Recent PIV experiments of Sabatino and Smith (2002) showed an increase in the streamwise velocity near the wall, leading to high skin friction values in this region. A comparison of the streamwise velocity profiles in the calmed region with the corresponding undisturbed laminar profiles that existed before the spot passage is shown in Figure 6. This confirms the occurrence of sweep event (positive u and negative v perturbations) behind a spot and helps the flow to recover its earlier non-inflectional laminar profile. If the disturbances in the spot wake are not damped (calming effect) then one can expect fresh breakdowns behind the spot tail and thereby a drastic reduction in the transition length. The existence of the 'calmed region' behind the turbulent spots induced by the periodic passing wakes in a turbine blade is found to reduce the profile loss. Stieger (2003) showed that the calmed region behind the turbulent spot was able to withstand more severe pressure gradients without separation.

3.2 Spot Celerities

3.2.1 Propagation Parameters

The streamwise positions of the front and rear interface of the spot are plotted against time on Figure 7. The respective velocities of the front and the tail of the spot are 0.767 u_∞ and 0.504 u_∞ in the near wall region (y = 0.25), 0.879 u_∞ and 0.512 u_∞ away from the wall (y = 2.6). The difference in the front interface velocity with the wall normal distance is due to the presence of the elongated overhang region i.e. inclination of the front interface of the spot.

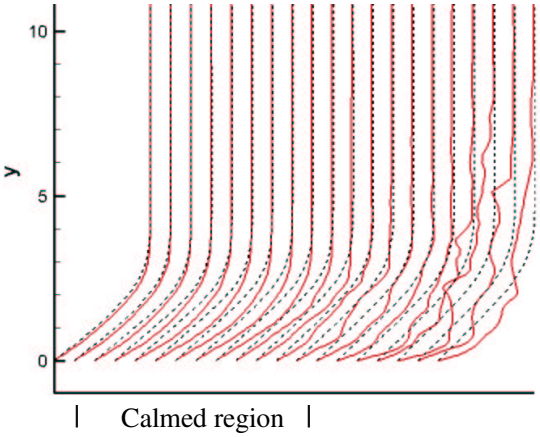

Figure 6: Streamwise velocity profiles in the calmed region (dashed line: corresponding undisturbed laminar profile)

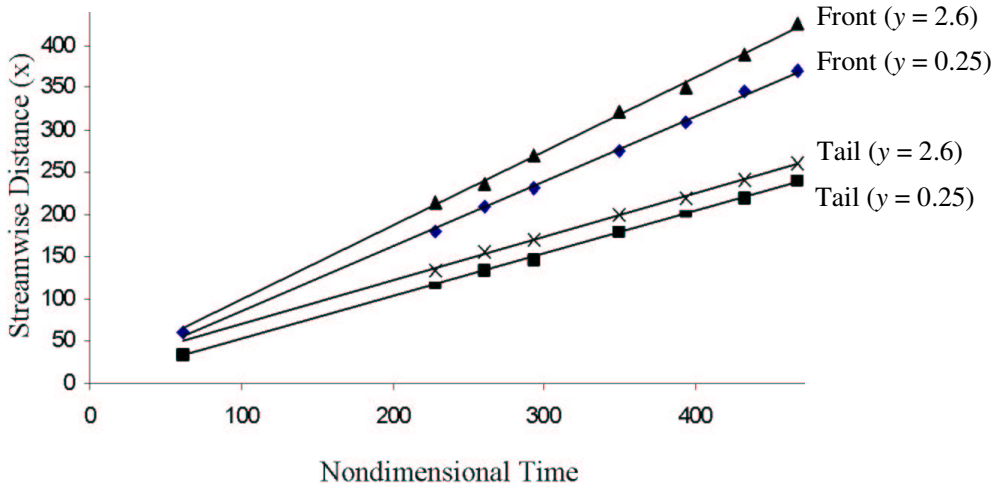

Figure 7: Axial locations of spot front, rear interface Vs Time

These calculated propagation speeds are in good agreement with the values of $0.9\,u_\infty$ and $0.5\,u_\infty$ reported in the literature.

3.2.2 Lateral Spreading

The lateral growth of a spot is highly dependent on the flow Mach number. The growth of a spot in the lateral direction is characterised by the half-spreading angle ($\phi=\tan^{-1}(b_h / (x_h-x_o))$), where b_h is the spot half-width, x_h is the streamwise location corresponding to maximum spot width and x_o is the origin of the spot. The half-width of the spot at various downstream locations is extracted and plotted against the corresponding streamwise locations in Figure 8. The lateral half-spreading angle of the spot is estimated to be 4.85 ± 0.2 degrees. This is in good agreement with the previous experimental studies at Mach 2.0 [4-7 degrees] (Fischer (1971).

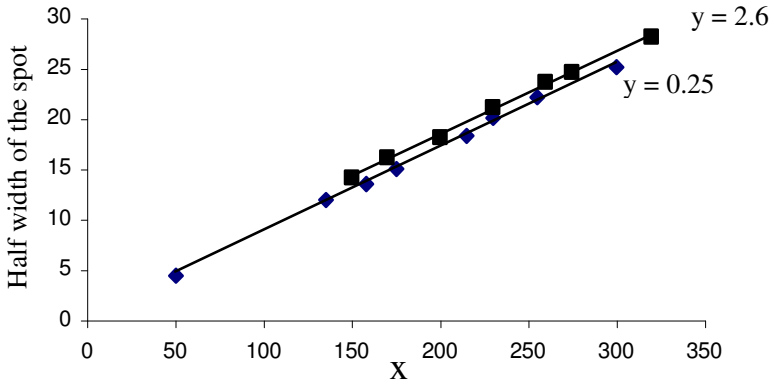

Figure 8: Spot half width vs Axial Distance (x)

3.3 Mean Flow and Turbulence Structure Inside the Spot

Spanwise-averaged flow properties (for $15 \le z \le 45$) at t = 468 are used to study the flow characteristics (see Figure 5). The shape factor ($H_k = \int \frac{u}{u_\infty}(1-\frac{u}{u_\infty})dy$) distribution along the flat plate is shown in Figure 9 and the mean wall friction velocity (u_τ) distribution in Figure 10. The maximum value of u_τ is around 0.055. The present grid resolution in viscous wall units was estimated to be $\Delta x^+ = \Delta x * u_\tau / \nu = 15-25$, and $\Delta z^+ = 7.5-12.5$ based on the maximum mean friction velocity at the wall, suggesting that the spot turbulence is properly resolved in the simulation.

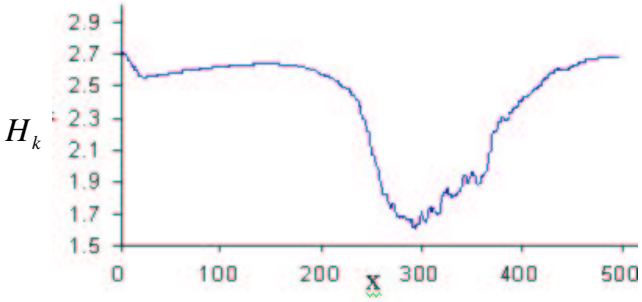

Figure 9: Shape Factor (H_k) distribution along the flat plate

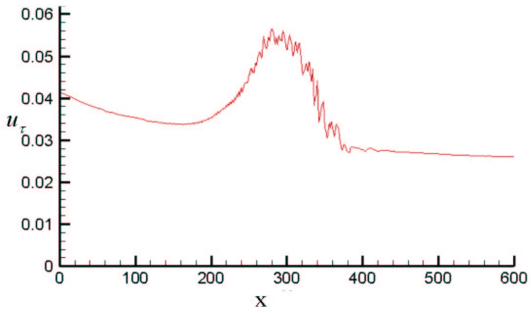

Figure 10: Friction velocity (u_τ) distribution

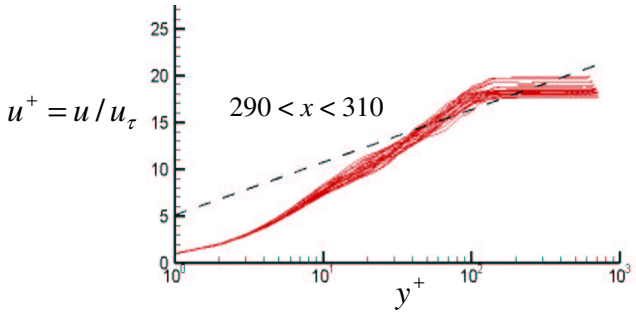

Figure 11: Streamwise velocity in wall units

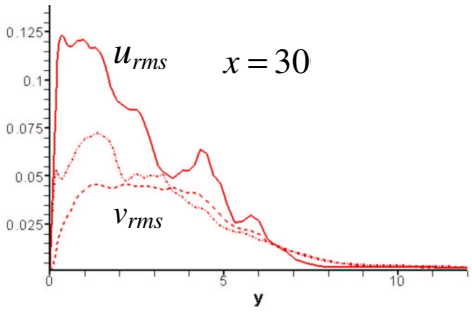

Figure 12: RMS velocity fluctuations

A semi-log plot of the mean velocity profiles at different streamwise locations clearly illustrates the existence of a developed turbulent region ($290 \le x \le 310$) inside the spot, which is compared with the law of the wall ($u^+ = 2.5*\ln(y^+) + 5.1$) (Figure 11). The corresponding distributions of the mean Reynolds normal stresses are shown in Figure 12. This confirms the development of a fully turbulent core region inside the spot. Figure 13 shows the comparison of mean c_f value in a turbulent spot with the laminar base flow case and the corresponding turbulent values of Coles (1953).

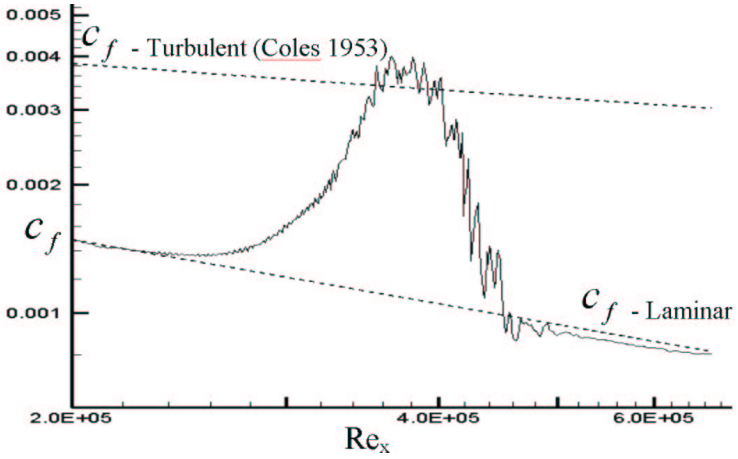

Figure 13: Skin friction (c_f) distribution along the flat plate at t=468

4 SPOT/SEPARATION BUBBLE INTERACTION (M2SSI)

Iso Mach contours in Figure 14 show the incident and reflected oblique shock chosen for the study of shock/transition interaction. An enlarged view of the laminar separation bubble and the skin friction distribution along the flat plate are shown in figure 15 and 16, respectively.

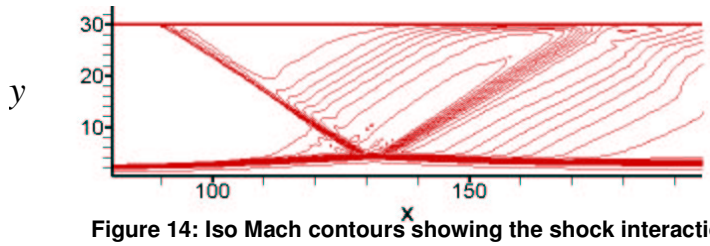

Figure 14: Iso Mach contours showing the shock interactions

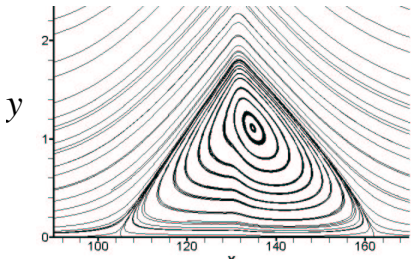

Figure 15: Enlarged view of the separation bubble

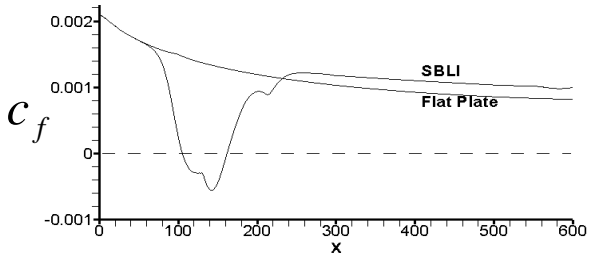

Figure 16: Skin friction distribution

The streamwise length of the separation bubble (100<x<160) is comparable to the length of the spot. Interaction of the oblique shock with the spot sub-structures can be clearly identified from Figure 17. Top

and side views of the spot and iso density contours at the peak plane (z = 30) are given in Figure 18 and 19 respectively. The height of the front overhang region of the spot is more than the height of the separation bubble. As a result the core region (middle) of the spot plays a major role in collapsing the bubble by "tunnelling" through the separation region (Figure. 20, 21.b). Due to the interaction a multitude of flow structures are introduced in the spot core region (Figure 21.a). To calculate the propagation parameters the axial locations of the spot head and tail are obtained from the integrated plan view of the wall-normal vorticity iso surface. The estimated convective speeds of the front and the rear interfaces of the spot are $0.831\,u_\infty$ and $0.384\,u_\infty$, respectively (Figure 22) against $0.879\,u_\infty$ and $0.504\,u_\infty$ for the M2S case studied earlier. The slow propagation of the rear half of the spot is an indication of the interaction with the separation bubble, which allows the spot to stay longer in the interaction zone. As a result of this the spot core has enough time to destabilise the surrounding laminar flow. This lead to a drastic increase in the spot lateral half-spreading angle from 5 degrees to 20 degrees (Figure 23).

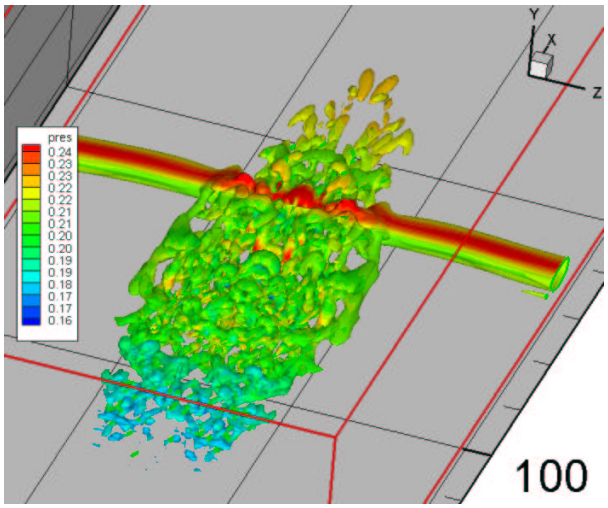

Figure 17: Spot sub-structures ($\prod = -0.003$) superimposed with the static pressure values (t = 169)

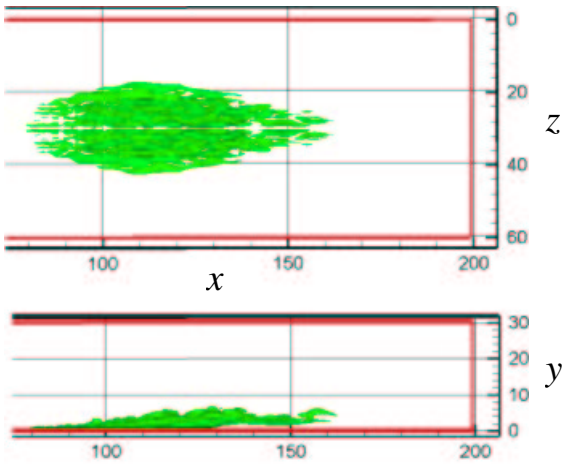

Figure 18: Iso surface of wall-normal vorticity (+0.06, - 0.06), (t=169)

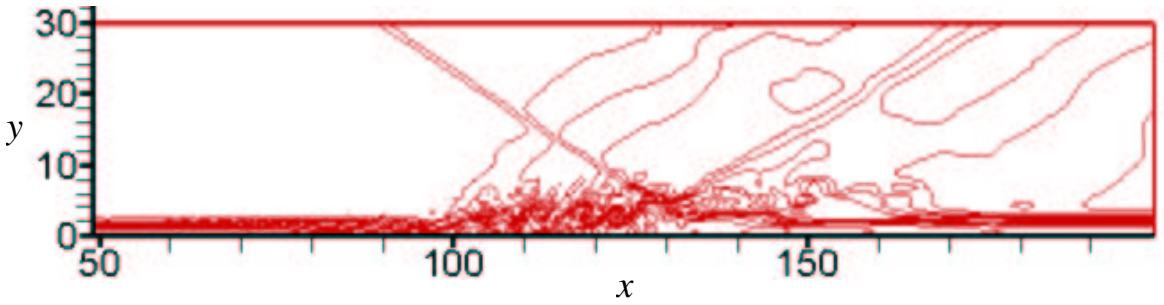

Figure 19: Constant density contours at the peak plane (*z*=30) (t = 169)

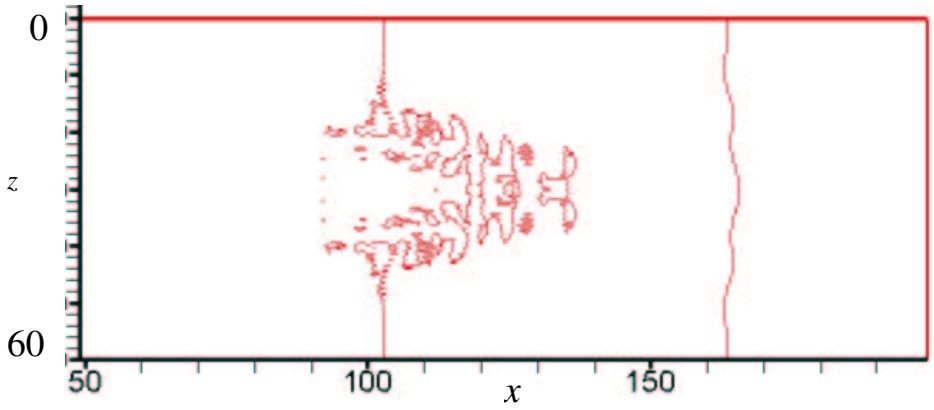

Figure 20: Zero contour of the wall shear $(\partial u/\partial y)_w = 0$ (t = 169)

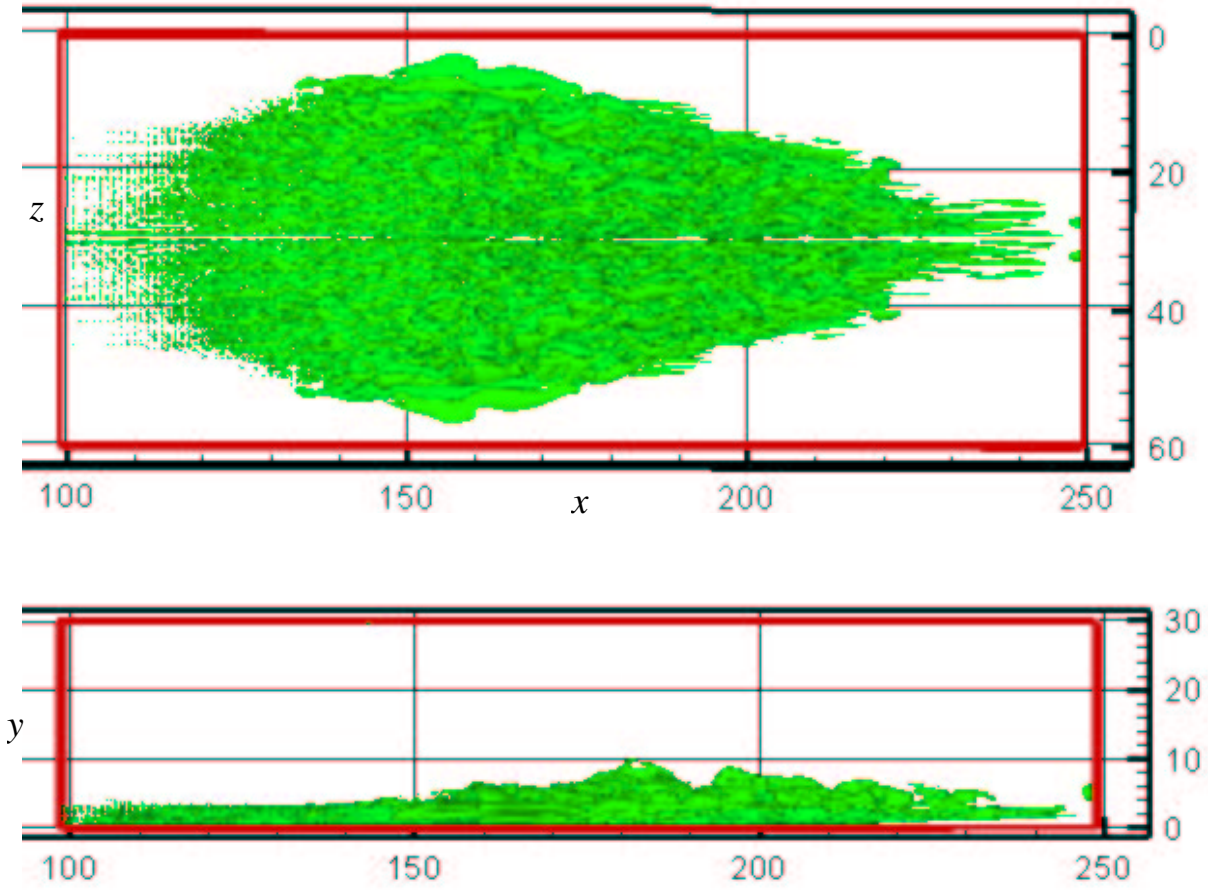

Figure 21.a: Top and side view of a well developed turbulent spot at t = 266 (shock impact at *x* = 137)

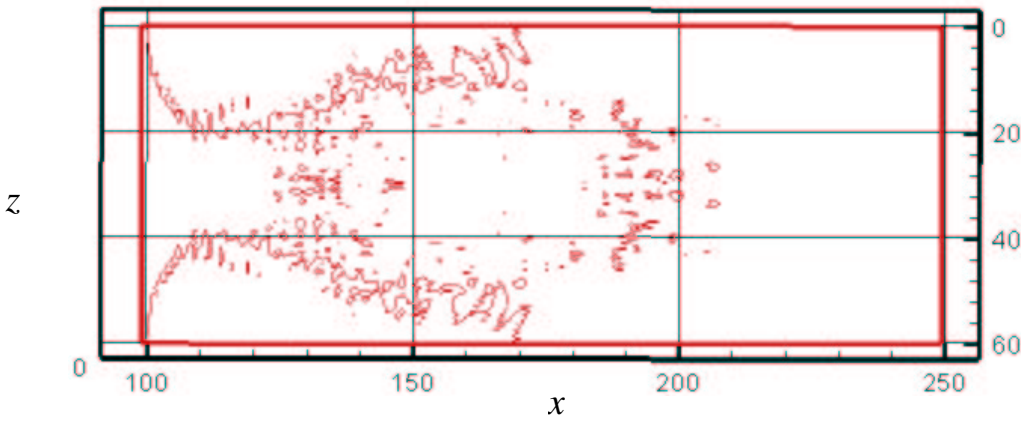

Figure 21.b: Zero contour of the wall shear $(\partial u/\partial y)_w = 0$ (t = 266)

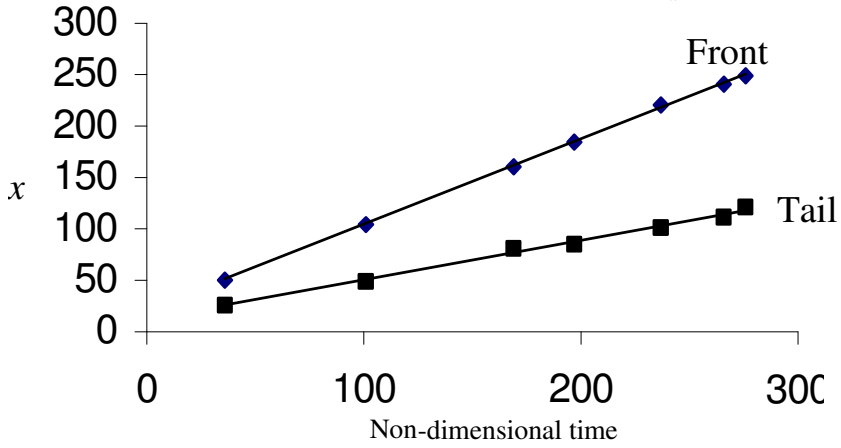

Figure 22: Axial locations of spot front and rear interface as a function of time

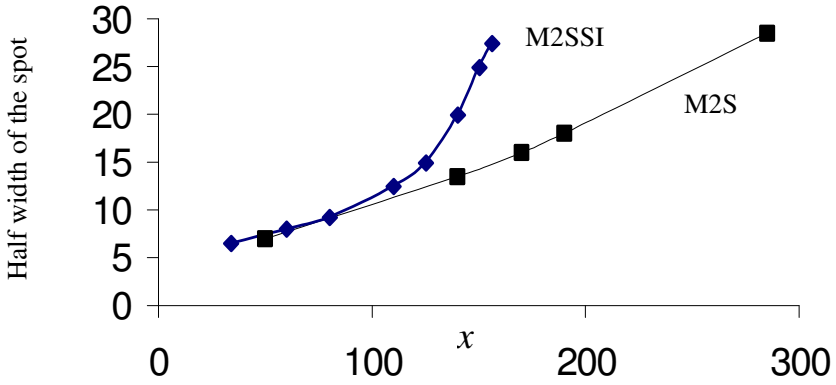

Figure 23: Spot half width as a function of axial distance (*x*)

The spanwise-averaged flow properties (for $20 \le z \le 40$) may again be used to study the flow characteristics inside the spot. The evolution of the span-averaged skin friction values during the spot/bubble interaction is shown in Figure 24. This clearly illustrates the complete collapse of the separation bubble at time t = 237 and t=266 (dashed line indicates separation). The span-averaged streamwise velocity profiles at the beginning, middle and end of the interaction zone are shown in Figure 25.

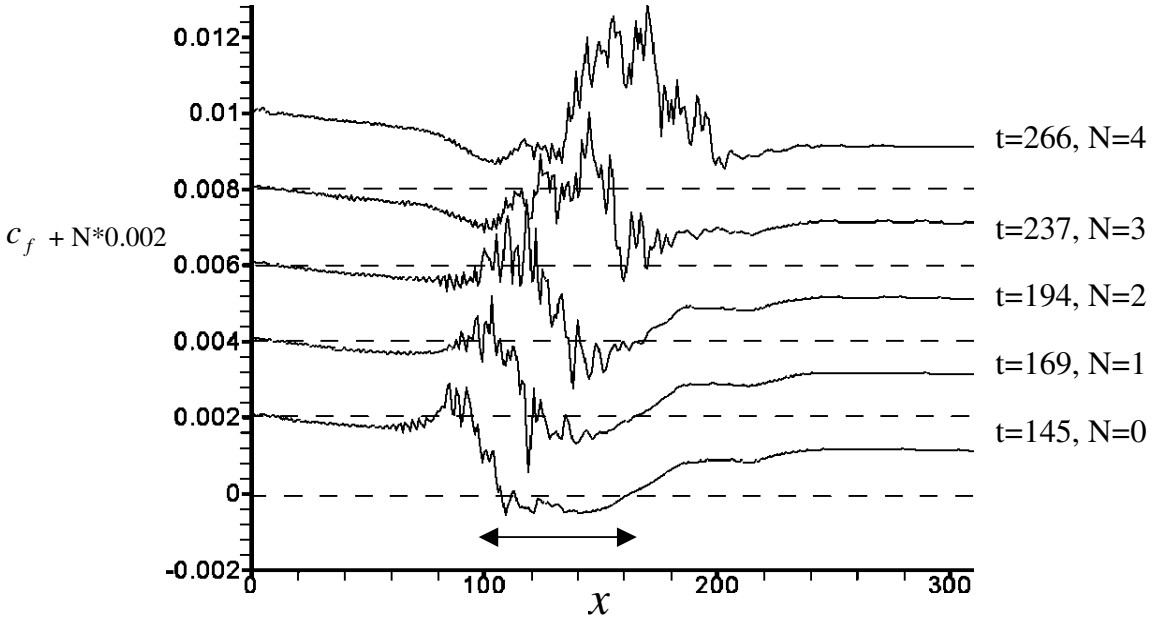

Figure 24: Skin friction distribution. The arrowed region (shows the bubble interaction zone for 100<x<165

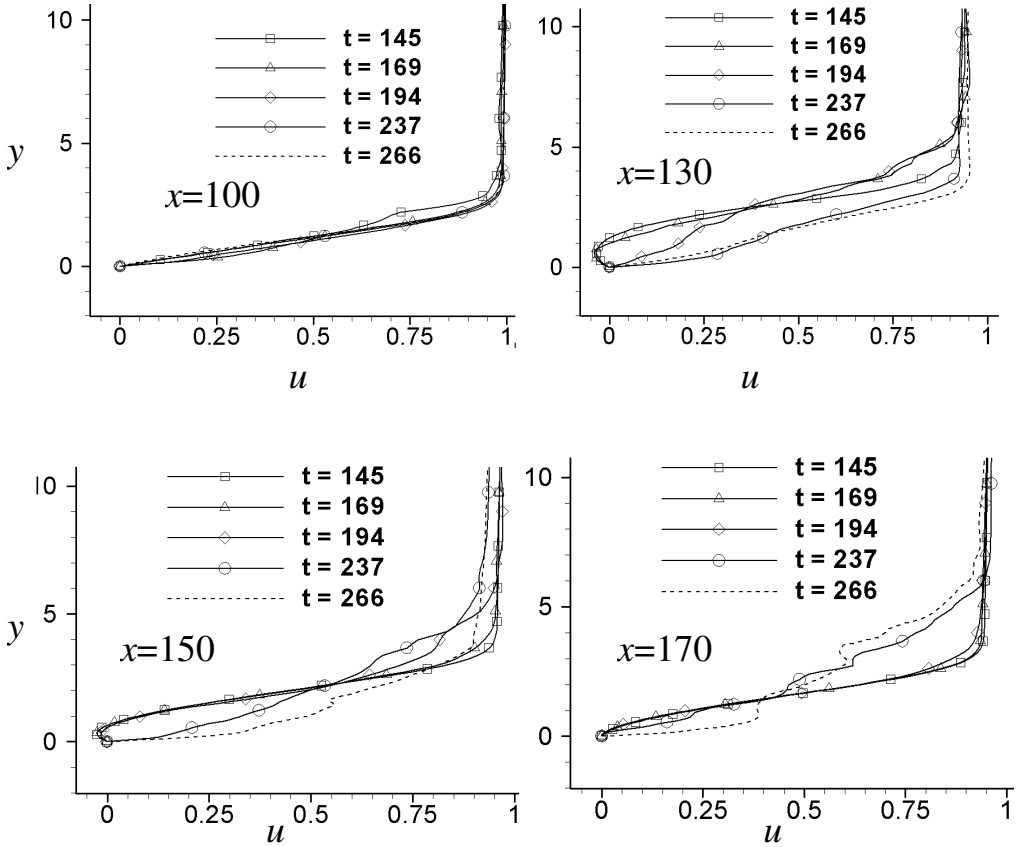

Figure 25: Streamwise velocity profiles in the interaction zone

5.CONCLUSIONS

The dynamics of a compressible turbulent spot and its interaction with a laminar separation bubble have been presented. A localised blowing trip mechanism was used to trigger a turbulent spot in a laminar base flow. Prior to the breakdown an array of hairpin structures and quasi-streamwise vortices were noticed inside the spot. A mature spot showed an arrowhead shaped front overhang region and a calmed region at the rear interface. The calculated flow properties inside the spot core region are found to be similar to a fully developed turbulent flow. The estimated spot growth rate and propagation parameters are consistent with previous experimental results and the effect of compressibility is to suppress the spot growth. The interaction of a turbulent spot with a shock-induced separation bubble considerably enhanced the spot spreading and drastic reduction in the transition length may occur due to the spot/separation bubble interactions. This is expected to play a major role in advancing the transition process in high-speed flows with strong compressibility effects. Further detailed analysis of the spot growth mechanism, compressibility effects and heat transfer characteristics will help in understanding the transition physics.

The authors would like to acknowledge the financial support of the European Space Agency (ESTEC) for this work.

6.REFERENCES

Carpenter, Nordstrom, Gottlieb, 1999, A stable and conservative interface treatment of arbitrary spatial accuracy. J. Computational Physics, 148: 341-365.

Coles D, 1953, Measurements in the boundary layer on a smooth flat plate in supersonic flow, PhD. Thesis, Caltech, Pasadena, California.

Dolling D S, 2001, Fifty years of shock-wave/boundary-layer interaction research: what next?, AIAA J., 39(8):1517-1531.

Fischer M C, 1972, Spreading of a turbulent disturbance, AIAA J., 10(7):957-959.

Gad-El-Hak M, Blackwelder R F, Riley R J, 1981, On the growth of turbulent regions in laminar boundary layers, J. Fluid. Mech., 110:73-95.

Kleiser L, Zang T A, 1991, Numerical simulation of transition in wall bounded shear flows, Ann. Rev. Fluid Mech., 23: 495 - 537.

Krishnan L, Sandham N D, 2004, Large eddy simulation of compressible turbulent spots, Advances in Turbulence X, H.I. Anderson & P.A Krogstad (Eds), CIMNE, Barcelona 2004, 467-471.

Mee D J, 2002, Boundary-Layer transition measurements in hypervelocity flows in a shock tunnel, AIAA J., 40(8): 1542 – 1548.

Narasimha R, 1985, The laminar-turbulent transition zone in the boundary layer. Prog. Aerospace Sci., 22: 81-111.

Perry A E, Lim T T, Tech E W, 1981, A visual study of turbulent spots, J. Fluid Mech., 104:387-405.

Sabatino D, Smith C R, 2002, Simultaneous velocity-surface heat transfer behavior of turbulent spots, Exp. in Fluids, 33: 13 - 21.

Sandham N D, Kleiser L, 1992, The late stages of transition to turbulence in channel. J. Fluid Mech., 245: 319 – 348.

Sandham N D, Li, Yee, 2002, Entropy Splitting for Higher-Order Numerical Simulation of Compressible Turbulence. J. Computational Physics, 178: 307-322.

Sankaran R, Sokolov M, Antonia R A, 1988, Substructures in a turbulent spot, J. Fluid Mech., 197:389-414.

Stieger R D, 2002, The effects of wakes on separating boundary layers in low pressure turbines, PhD. thesis, Cambridge University.

Zhong S, Kittichaikan C, Hodson H P, Ireland P T, 2000, Visualisation of turbulent spots under the influence of adverse pressure gradients, Exp. in Fluids, 28: 385-393.